LA-UR- 09-06179

Approved for public release; distribution is unlimited.

Title:	Increasing Runoff and Sediment Load from the Greenland Ice Sheet at kangerlussuaq (Sonder Stromfjord) in a 30-Year Perspective, 1979-2008
Author(s):	Sebastian H. Mernild, LANL; Glen Liston, Colorado State University; Bent Hasholt, University of Copenhagen; Konrad Steffen, University of Colorado; Michiel van den Broeke, Utrecht University; Daniel McGrath, University of Colorado; and Jacob Yde, University of Aarhus.
Intended for:	Journal of Hydrometeorology

Los Alamos
NATIONAL LABORATORY
EST.1943

Form 836 (7/06)

Increasing Runoff and Sediment Load from the Greenland Ice Sheet at Kangerlussuaq (Søndre Strømfjord) in a 30-Year Perspective, 1979–2008

SEBASTIAN H. MERNILD

Climate, Ocean, and Sea Ice Modeling Group, Computational Physics and Methods (CCS-2), Los Alamos National Laboratory, New Mexico, USA

GLEN E. LISTON

Cooperative Institute for Research in the Atmosphere, Colorado State University, Colorado, USA

BENT HASHOLT

Department of Geography and Geology, University of Copenhagen, DENMARK

KONRAD STEFFEN

Cooperative Institute for Research in Environmental Sciences, University of Colorado, Colorado, USA

MICHIEL van den BROEKE

Institute for Marine and Atmospheric Research, Utrecht University, HOLLAND

DANIEL McGRATH

Cooperative Institute for Research in Environmental Sciences,

University of Colorado, Colorado, USA

JACOB C. YDE

Center for Geomicrobiology, University of Aarhus, DENMARK, and

Bjerknes Centre for Climate Research, University of Bergen, NORWAY

Submitted 17 September 2009 to Journal of Hydrometeorology

Corresponding author address:

Dr. Sebastian H. Mernild

Climate, Ocean, and Sea Ice Modeling Group

Computational Physics and Methods (CCS-2)

Los Alamos National Laboratory,

Los Alamos, New Mexico 87545

USA

E-mail: mernild@lanl.gov

Abstract

This observation and modeling study provides insights into runoff and sediment load exiting the Watson River drainage basin, Kangerlussuaq, West Greenland during a 30 year period (1978/79–2007/08) when the climate experienced increasing temperatures and precipitation. The 30-year simulations quantify the terrestrial freshwater and sediment output from part of the Greenland Ice Sheet (GrIS) and the land between the GrIS and the ocean, in the context of global warming and increasing GrIS surface melt. We used a snow-evolution modeling system (SnowModel) to simulate the winter accumulation and summer ablation processes, including runoff and surface mass balance (SMB), of the Greenland ice sheet. Observed sediment concentrations were related to observed runoff, producing a sediment-load time series. To a large extent, the SMB fluctuations could be explained by changes in net precipitation (precipitation minus evaporation and sublimation), with 8 out of 30 years having negative SMB, mainly because of relatively low annual net precipitation. The overall trend in net precipitation and runoff increased significantly, while SMB increased insignificantly throughout the simulation period, leading to enhanced precipitation of 0.59 km^3 w.eq. (or 60%), runoff of 0.43 km^3 w.eq (or 54%), and SMB of 0.16 km^3 w.eq. (or 86%). Runoff rose on average from 0.80 km^3 w.eq. in 1978/79 to 1.23 km^3 w.eq. in 2007/08. The percentage of catchment outlet runoff explained by runoff from the GrIS decreased on average ~10%, indicating that catchment runoff throughout the simulation period was influenced more by precipitation and snowmelt events, and less by runoff from the GrIS. Average variations in the increasing Kangerlussuaq runoff from 1978/79 through 2007/08 seem to follow the overall variations in satellite-derived GrIS surface melt, where 64% of the variations in simulated runoff were explained by regional melt conditions on the GrIS. Throughout the simulation period, the sediment load varied from a minimum of 0.96×10^6 t y^{-1} in

1991/92 to a maximum of 3.52×10^6 t y^{-1} in 2006/07, showing an average increase of sediment load of 9.42×10^5 t (or 72%) throughout the period.

KEY WORDS Freshwater, Greenland Ice Sheet, Kangerlussuaq (Søndre Strømfjord), observations, runoff, sediment load, SnowModel

1. Introduction

Snow, glacier ice, and frozen ground influence runoff and sediment load processes throughout the Arctic. Significant responses in the structure and function of Arctic landscapes are likely, therefore, to occur in a warming climate. Rivers are dynamic geomorphic systems with adjustable forms that respond to climate-driven changes in runoff and sediment availability over a wide range of temporal scales (McNamara and Kane 2009).

The Greenland Ice Sheet (GrIS)—the largest terrestrial permanent ice- and snow-covered area in the Northern Hemisphere—is sensitive to changes in the climate. Observational and model-based studies of the GrIS have provided intriguing insights into a system-wide response to climatic change and the effects of a warmer and wetter climate on cryospheric and hydrologic processes. The response has been manifested by an increasing surface melt extent, peripheral thinning, accelerating mass loss, and freshwater runoff (e.g., Krabill et al. 2000, 2004; Janssens and Huybrechts 2000; Zwally et al. 2002; Johannessen et al. 2005; Fettweis 2007; Hanna et al. 2009; Mernild et al. 2009a; Richardson et al. 2009), indicating that mass loss of the GrIS may be responsible for nearly 25% of observed global sea rise in the past 13 years (Mernild et al. 2009b).

An important component of an ice sheet's surface mass balance is meltwater runoff, yet there are few high-resolution freshwater runoff observations at the periphery of the GrIS (e.g., Hag et al. 2002; Mernild et al. 2008a; Hasholt and Mernild 2009). A time series of river discharge from Kangerlussuaq (Søndre Strømfjord), West Greenland, has been recorded since 2007 and is of considerable importance to quantifying runoff from the ice sheet. These observations provide insight into the onset, duration, variation, and intensity of runoff, and the changes in intraannual and interannual hydrological response.

Quantitative information about the erosion rate caused by the GrIS, the sediment load, transport, and delivery to the open fjord/ocean is inadequate and generally absent, and the interrelationships among these components is not well understood. This lack of information is partly due to insufficient knowledge of basal conditions at the GrIS ice-bed interface and the effect of a lubricated interface that causes basal ice to slide over its bed. By combining available monitoring data and estimates from ungauged basins, Hasholt et al. (2006) indicated that the sediment load from Greenland to the Arctic Ocean and the Greenland Sea accounts for ~35–65% of total sediment transport from the Arctic. This indicates that glacial erosion is responsible for large sediment loads (e.g., Grunell et al. 1996; Bogen 1996; Hallet et al. 1997), which can exceed 1,000 t km^{-2} y^{-1}. The influence of a changing climate on the influx of sediment is likely not a simple function of the increased freshwater input. In addition to increased runoff, higher temperatures may further increase sediment yield through increased freeze-thaw processes of frozen ground and subglacial dynamics (e.g., Woo et al. 1992; Syvitski 2002). The magnitude of sediment flux, therefore, depends on both sediment availability and the presence of sinks (Hasholt et al. 2006). In many studies (e.g., Hasholt and Mernild 2006), however, the magnitude of the sediment load transported by a river is correlated with catchment runoff. Detailed observations of events and seasonal variations in the GrIS runoff and sediment load allow an understanding of the complexity of sub-basin-runoff sediment processes. Actually, sediment load during years with higher discharge could be enhanced by erosion and remobilization of sediments deposited in the proglacial area, between the GrIS and the drainage basin outlet, during years with low discharge. In general, understanding these situations and conditions will require additional observations and highlight the need to continue and expand GrIS runoff and sediment measurements.

It is essential to assess the impact of climate change on the GrIS, since the temperature rise in the northern latitudes is more pronounced than the global average; the observed increase is almost twice the global average rate of the past 100 years (IPCC 2007). Thus, the present state of the GrIS runoff and sediment load should be established to detect warning signs indicative of the ice sheet's future response. Projected climate scenarios suggest that the runoff and sediment load will increase in Arctic rivers (ACIA 2005). This study improves the quantitative understanding of freshwater runoff and sediment load from the Watson River drainage basin, near Kangerlussuaq, West Greenland.

In this study we applied a surface modeling system called SnowModel (Liston and Elder 2006a; Mernild et al., 2006a; Liston et al., 2007; Mernild et al. 2009c) to the Kangerlussuaq region for the 30-year period from 1978/79 through 2007/08. Our objectives were: (1) to simulate the variations and trends in the surface-water-balance components, including runoff, for the Kangerlussuaq catchment area; (2) to estimate the percentage of catchment runoff explained by GrIS runoff; (3) to compare satellite-derived GrIS melt-extent changes with the local Kangerlussuaq simulated runoff patterns; and (4) to estimate the variations and trends in sediment load to the fjord from the Kangerlussuaq drainage area based on modeled runoff.

2. Study area

a. Physical settings, meteorological stations, and climate

The Kangerlussuaq drainage area (6,130 km^2) is located on the west coast of Greenland (67°N latitude; 50°W longitude) (Figure 1a). The river outlet is located about 22–35 km downstream from the GrIS terminus, near Kangerlussuaq (Søndre Strømfjord), a town at the head of the Kangerlussuaq fjord. The outlet location is easily accessible and one of the best for

observing GrIS runoff and sediment load because of well-defined, stable bedrock cross sections and fully mixed water-column conditions; braided channels with unstable banks characterize most other river outlets in Greenland, making accurate runoff monitoring almost impossible. The upper part of the catchment area is dominated by the GrIS, and by bare bedrock, sparse vegetation cover, and river valleys in the lower parts.

Four meteorological stations are located within the simulation domain, with three of them located on the GrIS (Figure 1c and Table 1). Station Kangerlussuaq (hereafter referred to as Station K) (67°01′N, 50°42′W; 50 m a.s.l.; a Danish Meteorological Institute (DMI) WMO meteorological station) is located at the airport of the town Kangerlussuaq and is representative of the proglacial area. This station was moved in 2004 to its current location. No air temperature correction was made for the current study because the new station elevation is the same as the old site (for further information see Table 1). On the GrIS, three automatic weather stations are operated by Utrecht University. Stations S5 (67°06′N, 50°07′W; 490 m a.s.l.), S6 (67°05′N, 49°23′W; 1020 m a.s.l.), and S9 (67°03′N, 48°14′W; 1520 m a.s.l.) are all part of the K-transect, located on the ice sheet and representative of GrIS conditions (for further information about the K-transect stations see, e.g., van de Wal et al. 2005; van den Broeke et al. 2008a, 2008b, 2008c). The mean (1990–2003) equilibrium line altitude (ELA; defined as the elevation where the net mass balance is zero) in the region is ~1,530 m a.s.l., located near Station S9 (van de Wal et al. 2005; van den Broeke et al. 2008c).

The Kangerlussuaq region is considered Low Arctic according to Born and Böcher (2001). The SnowModel-simulated mean annual air temperature for the catchment (Figure 1) (1978/79–2007/08) is -10.9°C. Mean annual relative humidity is 64%, and mean annual wind

speed is 5.3 m s^{-1}. The corrected mean total annual precipitation (TAP) is 246 mm w.eq. y^{-1} (1978/79–2007/08) (corrected after Allerup et al. 1998, 2000; Mernild et al. 2007, 2008a).

3. SnowModel

a. SnowModel description

SnowModel (Liston and Elder 2006a) is a spatially distributed meteorological and snowpack-evolution modeling system. It consists of five submodels, with descriptions as follows. MicroMet (a quasi-physically-based meteorological distribution model) defines the meteorological forcing conditions (Liston and Elder 2006b). EnBal calculates the surface energy exchanges, including melt (Liston 1995; Liston et al. 1999). SnowPack simulates heat and mass transfer processes, and snow depth and water equivalent evolution (Liston and Hall 1995). SnowTran-3D is a blowing-snow model that accounts for snow redistribution by wind (Liston and Sturm 1998, 2002; Liston et al. 2007). SnowModel also includes a snow-data assimilation submodel (SnowAssim; Liston and Hiemstra 2008) that can be used to assimilate available snow measurements to create simulated snow distributions that closely match observed distributions when and where they occur (Liston et al. 2008). SnowModel was originally developed for glacier-free landscapes. For SMB studies in Greenland, SnowModel was modified to simulate (1) the glacier-ice melt after winter snow accumulation had ablated (Mernild et al. 2006a, 2007); (2) the influence of air temperature inversions on snowmelt and glacier SMB simulations where radiosonde data is present (Mernild and Liston 2009); and (3) the variable snow albedo as the snow ages and precipitation occurs (Mernild et al. 2009c). For this study, routines for temperature inversion were not included because of the lack of available radiosonde data in the area. SnowModel is a surface energy- and mass-balance model that produces first-order effects

of climate change; it does not include glacio-hydro-dynamic and glacio-sliding routines. The model produced runoff, is grid-cell runoff at each time step, summed over the Kangerlussuaq drainage domain, without any time-lag accounting between the grid-cell and basin outlet.

SnowModel has been used for a wide variety of snow and glacier landscapes in the United States, Norway, East Greenland, the Greenland Ice Sheet, and near-coastal Antarctica (see Liston et al., 2008 and Mernild and Liston 2009 and the references contained therein).

b. SnowModel input

To solve the SnowModel equations, the model requires spatially distributed fields of topography and land cover, and temporally distributed point meteorological data (air temperature, relative humidity, wind speed, wind direction, and precipitation), obtained from meteorological stations located within the simulation domain. High-resolution data were obtained from four meteorological stations: three stations (S5, S6, and S9) from the K-transect and one DMI WMO-operated station (Station K) (Figure 1c, Table 1). The simulations span the 30-year period 1 September 1978 through 31 August 2008, approximately following the annual GrIS mass-balance year and coinciding with the period of available passive microwave satellite-derived GrIS melt extent data. The simulations were performed on a daily time step, even though blowing snow, snowmelt, and ice melt are threshold processes that may not be accurately represented by daily time-step simulations, since daily-averaged atmospheric-forcing variables, in contrast to hourly data, smoothed the meteorological driving data.

For 2003/04 through 2006/07, meteorological input data from Stations K, S5, S6, and S9 were used, and for the period before (1978/79 through 2002/03) and after (2007/08) that time, only data from Station K were used. Mean monthly lapse rates (September 2003 through August

2007) were defined for the model simulations based on air temperature observations along a transect drawn between Stations S5, S6, and S9 (for further information see Mernild et al. 2009d).

Across the Arctic, it is well known that precipitation gauges significantly underestimate both liquid and solid precipitation because of aerodynamic errors at the gauging stations, especially under windy and cold conditions (e.g., Yang et al. 1999; Liston and Sturm 2002, 2004; Serreze and Barry 2005). Precipitation at the DMI meteorological station (Station K; Figure 1c, Table 1) was defined by correcting Helman–Nipher shielded gauge observations following Allerup et al. (1998, 2000).

Greenland topographic data for model simulations were provided by Bamber et al. (2001), who applied "correction" elevations derived by satellite imagery to an existing radar-altimetry digital elevation model (DEM). The image-derived correction was determined from a high-resolution (625 m) grid of slopes inferred from the regional slope-to-brightness relationship of 44 AVHRR images covering all of Greenland (Scambos and Haran 2002). For model simulations, this DEM was aggregated to a 500-m grid-cell increment and clipped to yield a 750-by-580-km simulation domain (435,000 km^2; the Kangerlussuaq region) (Figure 1b). The GrIS terminus was confirmed or estimated by using satellite images (Google Earth, Image 2009). Each grid cell within the domains was assigned a USGS Land Use/Land Cover System class, according to the North American Land Cover Characteristics Database, Version 2.0 (available on-line at [http://edcdaac.usgs.gov/glcc/na_int.html] from the USGS EROS Data Center's Distributed Active Archive Center, Sioux Falls, South Dakota, USA). The snow-holding depth in SnowModel (the snow depth that must be exceeded before snow can be transported by wind) was assumed constant. A variable snow albedo was used (Mernild et al. 2009c), and when the

snow was ablated, GrIS surface ice conditions were used. Albedo was assumed at 0.4 for ice; however, the GrIS ablation area is characterized by lower albedo on the margin and an increase in albedo toward the ELA, where a veneer of ice and snow dominate the surface (Boggild et al. 2006). The emergence and melting of old ice in the ablation area create surface layers of dust (including black carbon particles) that originally were deposited with snowfall higher on the ice sheet. This debris cover often is augmented by locally derived windblown sediment. Particles on or melting into the ice change the area-average albedo, increasing the melt rate. User-defined constants for SnowModel are shown in Table 2 (for parameter definitions, see Liston and Sturm 1998, 2002).

c. SnowModel calibration, verification, and uncertainty

To assess the general performance of the SnowModel-simulated distributed meteorological data and snow evolution, snow and ice surface melt, glacier net mass-balance, and snow and ice processes, simulated values were tested against independent observations. SnowModel/MicroMet-distributed meteorological data have been compared against independent Greenland meteorological station data both on and outside the GrIS, indicating respectable (84–87% variance for air temperature, 49–55% for wind speed, 49–69% for precipitation, and 48–63% for relative humidity) representations of meteorological conditions (for further information, see Mernild et al. 2008b; Mernild and Liston 2009). Few verification observations for *in situ* snow evolution, snow and ice surface melt, and glacier net mass balance are available in Greenland. Therefore, SnowModel accumulation and ablation routines were tested qualitatively (by visual inspection) and quantitatively (cumulative values and linear regression) using independent *in situ* observations on snow pit depths; glacier winter, summer, and net mass

balances; depletion curves; photographic time lapses; and satellite images from in and outside the GrIS (e.g., Mernild et al. 2006a, 2007, 2009a). A comparison performed between simulated and observed values indicates a 7% maximum difference between modeled and observed snow depths, glacier mass balance, and snow cover extent.

To assess the winter and summer model performance for this Kangerlussuaq study, the end-of-winter (31 May; recognized as the end of the accumulation period) simulated snow depth was compared with Station S9 observed snow depth, and the simulated cumulative summer (June through August) runoff was compared with observed catchment outlet runoff entering directly into Kangerlussuaq Fjord. Station S9 snow depth was measured 31 May, and used to verify and adjust the SnowModel-simulated snow depth (Mernild et al. 2009d). Using Station K precipitation, the simulated snow depth was on average overestimated by ~50% (400 mm w.eq.) (2003/04–2006/07). Therefore, an iterative precipitation-adjustment and convergence scheme following Liston and Hiemstra (2008) was implemented which yielded a simulated Station S9 snow depth on 31 May that was within 1% of the observed snow depth (for further information, see Mernild et al. 2006a, 2009d; Liston and Hiemstra 2008). Catchment outlet runoff was observed for the 2007 and 2008 runoff seasons (Mernild et al. 2008a; Mernild and Hasholt 2009). Stage and discharge measurements were used to develop a stage-discharge relationship (R^2=0.91, p<0.01; where p is level of significance) (linear regression; hereafter all regressions will be linear) (Mernild et al. 2009d) and to convert stage measurements into river-runoff time series. The relationships are expected to have an accuracy of 10–15% (Mernild and Hasholt 2009). After runoff adjustment and verification, the difference in simulated and observed runoff was within 1% for 2006/07 and 10% for 2007/08 (the observed values are included in Figure 3a) (Mernild et al. 2009d).

Our SnowModel methodology provided estimates of the Kangerlussuaq cumulative runoff that agreed well with observed values. Nevertheless, it is important to keep in mind the limitations of these SnowModel results: (1) model simulations were tested against a sparse observational dataset; and (2) uncertainties are likely influenced by processes not yet represented within the modeling system; for example, routines for simulating changes in GrIS area, size, and surface elevation in response to glacier dynamic and sliding processes are not accounted for by SnowModel. In addition, runoff from geothermal heating/melting was not included in the calculations. Moreover, changes in GrIS storage based on supraglacial, englacial, subglacial, and proglacial storage, internal meltwater routing, and evolution of the internal runoff drainage system are not calculated in SnowModel, even though they may have important influences on runoff.

4. Suspended sediment

Suspended sediment concentration (SSC) was determined at the Kangerlussuaq outlet by filtering ten 0.5 litre water samples that were collected weekly and manually in 2008 under the Watson Bridges at the Kangerlussuaq drainage-area outlet. The water samples were filtered through pre-weighed Whatman GF/F filters with a nominal retention diameter of 0.7 microns. The filters were dried at a temperature of 65°C and re-weighed. Hereafter, filters were burned at 550°C to determine weight loss of ignition. After subtraction of the clean-filter weight, the concentration was determined by dividing the two weights with the sample volume; results were given in mg L^{-1}. Because of the rather large concentration values, the accuracy of analyzed concentration values will most often be better than ±5%.

A discharge–SSC relationship (SSC = 4.1discharge + 859.3, R^2=0.81, p<0.01) was established (expecting to have an accuracy of 10–15%), and converted into sediment-load time series for the simulation period. The relationship is expected to be valid: 1) outside (below and above) the interval of observed discharge (Figure 2); and 2) without taking into account the daily variation in hysteresis in the discharge-SCC relationship. SSC was further determined by samples taken 150 and 700 m upstream from the outlet at the riverbank. Unfortunately, the upstream samples only represent a part of the total sediment load (mostly wash load) because of the variation in concentration both laterally and vertically in the river cross section. However, at the outlet, the samples represent total sediment load based on fully mixed water-column conditions because of the super critical flow and the formation of the hydraulic jumps and "haystacks" underneath the bridges. In Figure 2, the discharge water-sample relationships are illustrated, indicating a R^2 value of 0.81 (p<0.01) and 0.03 (p<0.10) for the outlet and upstream samples, respectively. The average concentration of the upstream samples is significantly different (97.5%-quantile) and ~30% lower than at the outlet. This indicates that the outlet sediment load is strongly controlled by the bedload, more than the suspended sediment load. Using the underestimated sediment data from upstream, therefore, will miscalculate the sediment load to the fjord from the Kangerlussuaq drainage area.

5. Results and discussion

Throughout the year, different surface processes such as snow accumulation, redistribution, blowing-snow sublimation, surface evaporation, and surface melt affect the GrIS surface mass balance (SMB) and the high-latitude water balance, including runoff. The yearly water balance equation for the catchment can be described by

$$P - (ET+SU) - R \pm \Delta S = 0 \pm \eta \quad (1)$$

where P is the precipitation input from snow and rain (and possible condensation) (net precipitation: precipitation minus evapotranspiration and sublimation), ET is evapotranspiration (liquid-to-gas phase [atmosphere] flux of water vapor), SU is sublimation, including blowing-snow sublimation (snow blowing; solid-to-gas phase with no intermediate liquid stage), R is runoff, and ΔS is change in storage (ΔS is also referred to as the SMB) from changes in glacier ice storage and snowpack storage. Glacier storage also includes changes in supraglacial storage (lakes, pond, channels, etc.), englacial storage (ponds and the water table), and subglacial storage (cavities and lakes); these glacier storage components were not accounted for in this study. Here, η is the water balance discrepancy (error). The error term should be 0 (or small) if the major components (P, ET, SU, R, and ΔS) have been determined accurately. Here, a change in storage is calculated by the residual value.

Sublimation may play an important role in the high-latitude hydrological cycle during the year. Previous GrIS studies (e.g., Box and Steffen 2001; Mernild et al. 2008b) have shown that as much as 17–23% of the annual precipitation was returned to the atmosphere by sublimation. In Arctic North America, studies by Liston and Sturm (1998, 2004), Essery et al. (1999), and Pomeroy and Essery (1999) indicated that 5–50% of the annual solid precipitation was returned to the atmosphere by sublimation. Blowing-snow sublimation rates are mainly dependent upon air temperature, humidity deficiency, wind speed, and particle-size distribution (Schmidt 1972, 1982; Tabler 1975; Pomeroy and Gray 1995; Liston and Sturm 2002). For the Kangerlussuaq catchment (1978/79–2007/08), modeled annual sublimation averaged 0.33(±0.08) $km^3\ y^{-1}$, or

~17% of the annual precipitation input. In the entire Kangerlussuaq simulation domain, sublimation played a lesser role in the surface moisture budget. Simulated evaporation, however, averaged 0.31(±0.07) $km^3\ y^{-1}$, indicating that total loss from sublimation and evaporation was 0.64(±0.16) $km^3\ y^{-1}$, which equalled ~33% of the annual precipitation input. Loss from transpiration from the proglacial area between the GrIS terminus and Kangerlussuaq Fjord was not taken into account for the Kangerlussuaq simulations since vegetation in this area is so limited.

Figure 3a presents surface-modeled water balance components (Equation 1) for the Kangerlussuaq drainage area from 1978/79 through 2007/08. The SMB was governed by accumulation (precipitation) and by ablation (evaporation, sublimation, and runoff). Net accumulation occurred over the GrIS interior (above the ELA (equilibrium line altitude) approximately located from 1,640 m a.s.l. to the south to 600 m a.s.l. to the north of the GrIS (see e.g., Zwally and Giovinetto 2001, Box et al. 2004, Mernild et al. 2008a), while net surface ablation dominates the terminus/low-lying parts of the GrIS. Statistically significant relationships exist between net precipitation and SMB, and runoff and SMB: The interannual variability in net precipitation and runoff causes sizeable SMB fluctuations with correlations of R^2=0.51, p<0.01, and R^2=0.22, p<0.01, respectively. Surface mass-balance fluctuations were largely tied to changes in net precipitation processes, and less to summer air temperatures (Table 3). Throughout the simulation period, SMB varied from -0.39 (1979/80) to 0.97 km^3 w.eq. (1982/83), averaging 0.26(±0.34) km^3 w.eq. y^{-1}. In 8 out of 30 simulation years, the SMB was negative (Figure 3a; Table 3), mainly because of relatively low net precipitation. For the 1978/79–2007/08 simulations, 1979/80, 1989/90, 1984/85, and 1983/84 were the first, second, third, and fourth lowest-precipitation years, respectively, and 1979/80, 1989/90, 1998/99, and

1984/85 were the first, second, third, and fourth lowest-SMB years, respectively. The year 1982/83 had the highest positive SMB of 0.97 km^3 w.eq., because of relatively high net precipitation (1.60 km^3 w.eq.) and low runoff (0.62 km^3 w.eq.). For the years 1998/99 and 2006/07, however, the low SMB was based on high runoff values, where 2006/07 and 1998/99 had the first and second highest runoff, respectively (Table 3). For 2006/07, the runoff was 1.76 km^3 w.eq.; approximately 75% higher than the average runoff for the period 1978/79 through 2007/08 (except for 2006/07) of 0.99(±0.21) km^3 w.eq. y^{-1}. The overall trend in Figure 3a illustrates a significant increase of both net precipitation and runoff, leading to enhanced average precipitation of 0.59 km^3 w.eq. (or 60%) (R^2=0.33, p<0.01) and runoff of 0.43 km^3 w.eq. (or 54%) (R^2=0.31, p<0.01) during the 30-year time period. The runoff rose on average from 0.80 km^3 w.eq. in 1978/79 to 1.23 km^3 w.eq. in 2007/08. For the SMB, however, the increase indicated an insignificant trend (R^2=0.02, p<0.10), leading to an enhanced average gain of mass of 0.16 km^3 w.eq. (or 86%), largely due to changes in precipitation. Since storm tracks determine the distribution of precipitation across Greenland (e.g., Hansen et al., 2008), the average increase in precipitation in the Kangerlussuaq area is most likely due to changes of the passage of low pressure systems around Greenland.

Figure 3b presents the simulated outlet runoff from the Kangerlussuaq drainage area from 1978/79 through 2007/08, subdivided between runoff originating from the GrIS or precipitation and snowmelt. The percentage of catchment runoff explained by runoff from the GrIS varied from a maximum of 70% in 1979/80 to a minimum of 36% in 2004/05, averaging 51(±9)% (Figure 3b), where 70% of the explained variance in catchment runoff was from GrIS runoff (Figure 3c). Further, the variation in percentage of catchment runoff explained by the GrIS was significantly influenced by changes in SMB (R^2=0.65, p<0.01), showing that years with high

percentage values correspond to years with negative SMB and vice versa. The overall trend (R^2=0.11, p<0.05, significant) for the period 1978/79 through 2007/08 indicated that the percentage of catchment runoff explained by the GrIS decreased on average ~10% from 55% (1978/79) to 45% (2007/08). This decrease means that the catchment runoff throughout the simulation period was influenced more by precipitation and snowmelt events, and less by runoff from the GrIS.

Seasonal variation in runoff is illustrated in Figures 4a and 4b, both for catchment runoff and GrIS runoff for the year, with the minimum (1991/92) and maximum (2006/07) cumulative runoff. During winter (September/October through May/June), no runoff events where simulated for the Kangerlussuaq drainage area for the period 1978/79 through 2007/08. For the year 2006/07, the first day of modeled runoff occurred at the end of May. Visual observations from 2006/07 and 2007/08 indicated that outlet runoff normally starts around mid/late April (Hasholt and Mernild 2009), approximately 2–3 weeks before simulated runoff, and stops late September to mid-October, which was in accordance with simulated values. In the early melt period (April and May), runoff was controlled mainly by snowmelt, whereas later in the season (mid-July and August) when the seasonal snow cover had largely melted, runoff was dominated by glacier-ice melt. When surface melting was defined by SnowModel, meltwater is assumed to run as "runoff" instantaneously when the surface consists of glacier ice. When snow cover was present, the SnowPack runoff routines take retention and internal refreezing into account when meltwater melts at the surface and penetrates the snowpack. These routines have an effect on the runoff lag time and the amount of runoff. If no retention/refreezing routines were included in SnowModel, the initial seasonal runoff would occur up to, e.g., 81 days before, and the Kangerlussuaq runoff

would be overestimated up to ~65% (based on values from 2006/07 and 2007/08) (Mernild et al. 2008a).

Surface-modeled water-balance components for the Kangerlussuaq drainage area were compared with a regional GrIS area surface study from 1995/96 through 2006/07 (Mernild et al. 2009b). For Kangerlussuaq, the average simulated runoff of 1.02(±0.25) km^3 y^{-1}, equals 2.5‰ of the average GrIS surface runoff of 397(±62) km^3 y^{-1}. The Kangerlussuaq runoff trend, illustrated in Figure 3a, is in accordance with the regional runoff trend for the GrIS; both indicate increasing runoff. However, the trend in regional GrIS precipitation was almost zero, while GrIS SMB decreased, leading to enhanced average regional GrIS mass loss. The average regional GrIS SMB pattern was different from the local trends at Kangerlussuaq, West Greenland, probably because the characteristics of Greenland caused considerable contrast in its weather conditions. Local climatic trends often differ over short distances due to the complex coastal topography, elevation gradients, distance from the coast, marginal glaciers, and the presence of the GrIS.

In Figure 5a, a time series of the satellite-derived GrIS total melt area is shown, together with local Kangerlussuaq runoff from 1978/79 to 2007/08. For the simulation period, the GrIS melting area increased significantly ~60% on average (Richardson et al. 2009), where the year 2007 indicated record GrIS surface-melt extent according to observations (Mote 2007; Tedesco 2007; Richardson et al. 2009). The melting intensification occurred simultaneously with the increase in local Kangerlussuaq runoff. For Kangerlussuaq, the runoff significantly increased by ~55% from 1978/79 through 2007/08 (R^2=0.30, p<0.01), which is almost identical with the relative changes in the GrIS total melt area. Further, for the year 2006/07, record modeled Kangerlussuaq runoff of 1.76 km^3 w.eq. occurred (Table 3). The average variations in the

increasing Kangerlussuaq runoff from 1978/79 through 2007/08 closely follows the overall variations in the satellite-derived GrIS surface melt (Figure 5a), where 64% of the simulated runoff variation was explained by regional melt conditions (Figure 5b). However, the simulated runoff does not take into account year-to-year runoff variations due to all possible changes in GrIS freshwater storage (see Equation 1). Observations from the Kangerlussuaq drainage by Sugden et al. (1985), Roberts (2005), and Mernild et al. (2009), for example, indicated that sudden short-lived glacial outburst floods (jökulhlaups) occurred. Each year in 1983 and 1984, a short-lived jökulhlaup event was observed, and again in 2007 and 2008 based on water stored on the GrIS surface, internally, or in ice-dammed lakes. While SnowModel does not simulate sudden releases of internal GrIS water storage, such events certainly influence peak seasonal runoff, isolated and rapid discharge events, and river dynamics and their impact on transporting sediment to the fjord, even though jökulhlaups and similar discharge occurrences likely only account for a small percentage of the cumulative runoff.

Time series of modeled suspended sediment load from the Kangerlussuaq drainage area are shown in Figure 6. Since the sediment load was treated as a simple linear function of the discharge (runoff) input to the fjord (Figure 2), the sediment trend was increasing significantly as well (R^2=0.30, p<0.01) for the period 1978/79 through 2007/08. In a warmer climate, the increasing thaw processes and changes in GrIS subglacial dynamics may increase the sediment yield further. However, for the simulation period the average increase in sediment load was 9.42×10^5 t (or 72%). Throughout the simulation period, the sediment load varied from 0.96×10^6 t (1991/92) to 3.52×10^6 t (2006/07), averaging $1.77(\pm0.52)\times10^6$ t y^{-1} (Figures 4c, 4d, and 6; Table 3). For Kangerlussuaq the average simulated sediment load of 1.77×10^6 t y^{-1}, equals between ~0.3–1.5% of the average Greenland sediment load of $116–586\times10^6$ t y^{-1} to the Arctic Ocean and

the Greenland Sea estimated by Hasholt et al. (2006). In Figures 4c and 4d, the seasonal variation in sediment load is illustrated for the catchment outlet for the year with the minimum (1991/92) and the maximum (2006/07) cumulative sediment load, indicating that daily values above 3.0×10^{8} kg d^{-1} during periods with peak runoff might occur.

Understanding water movement and the hydrologic response within and below the GrIS is intrinsically complex and not well understood. It involves the liquid phase (water) moving through the solid phase (ice) at the melting temperature while the ice is deformable, allowing englacial and subglacial conduits to change size and shape. Furthermore, efforts to model the links between the GrIS's mass balance, its dynamic processes, changes, internal drainage, runoff, and subglacial sliding and erosion, including the Kangerlussuaq drainage area, still suffer from substantial uncertainties and limitations. These uncertainties and limitations are related partly to insufficient knowledge of englacial routing and basal conditions at the GrIS ice-bed interface, and the effect from a lubricated interface that causes basal ice to slide over its bed. How the increasing volume of surface meltwater, due to increasing melt content, affects the dynamics, the subglacial sliding processes, and the erosion rates are still unanswered questions. This formidable question promises to be at the frontier of Arctic and climate-change science investigations in the coming years. A long-term perspective using runoff modeling of Kangerlussuaq from 1978/79 to 2007/08 is an initial step in helping us to provide new information on runoff that exits a part of the GrIS and the effects of a warmer and wetter climate in a time of climatic change.

6. Summary and conclusion

Thirty years of SnowModel simulations of runoff and sediment load from a sector of the GrIS—the Kangerlussuaq drainage area—were provided for the period 1978/79 through 2007/08, a period of climatic change with effects of a warmer and wetter climate. This simulated time series yielded useful insights into present conditions on the ice sheet and the interannual variability of SMB and runoff. The simulations indicate fluctuations in SMB that were largely tied to changes in net precipitation, showing 8 out of 30 years had negative SMB mainly because of relatively low annual net precipitation. Further, the overall trend in both net precipitation and runoff increased significantly, resulting in a ~10% reduction in the percentage of catchment runoff explained by runoff from the GrIS. The increasing Kangerlussuaq runoff is strongly correlated with the overall pattern of the satellite-derived GrIS surface melt. Since modeled sediment load was linearly related to runoff, the sediment load further increased from 1978/79 through 2007/2008. Efforts to model the link between the GrIS SMB, its dynamic processes, changes, internal drainage, runoff, and subglacial sliding and erosion, suffer from substantial uncertainties and limitations. This is true of the GrIS in general, and the Kangerlussuaq drainage area targeted by the analysis presented herein. These uncertainties and limitations are related partly to insufficient knowledge of basal conditions at the ice-bed interface of the GrIS, and the effect of increasing meltwater production influencing the lubricated interface that causes basal ice to slide over its bed.

Acknowledgments

Special thanks to the Institute for Marine and Atmospheric Research, Utrecht University, for the use of observed snow depth data and meteorological data from stations related to the K-transect on the Greenland Ice Sheet; to the Cooperative Institute for Research in Environmental

Sciences, University of Colorado, for the use of satellite data; and finally to the Department of Geography and Geology, University of Copenhagen for use of observed runoff data and suspended sediment data. This work was supported by grants from the University of Alaska Presidential IPY Postdoctoral Foundation, the Los Alamos National Laboratory, Kommisionen for Videnskabelige Undersøgelser i Grønland (KVUG), and the Danish Natural Science Research Council (SNF), and was carried out during the first author's IPY Post Doctoral Program at the University of Alaska Fairbanks.

References

ACIA, 2005. Arctic Climate Impact Assessment. Cambridge University Press, 1042 p.

Allerup, P., H. Madsen, and F. Vejen, 1998. Estimating true precipitation in arctic areas. *Proc. Nordic Hydrological Conf.,* Helsinki, Finland, Nordic Hydrological Programme Rep. 44: 1–9.

Allerup, P., H. Madsen, and F. Vejen, 2000. Correction of precipitation based on off-site weather information. *Atmos. Res.,* 53: 231–250.

Bamber, J., S. Ekholm, and W. Krabill 2001. A new, high-resolution digital elevation model of Greenland fully validated with airborne laser altimeter data. *J. Geophys. Res.*, 106(B4): 6733–6746.

Bogen, J. 1996. Erosion and sediment yield in Norwegian rivers. In: Erosion and Sediment Yield: Global and regional Perspectives, D.E. Walling and B. W. Webb (eds.). *IAHS* 236: 73–84.

Boggild, C. E., S. G. Warren, R. E. Brandt, and K. J. Brown 2006. Effects of dust and black carbon on albedo of the Greenland ablation zone. Abstract: American Geophysical Union, Fall Meeting 2006, abstract #U22A-05.

Born, E. W., and J. Böcher, 2001. *The Ecology of Greenland.* Ministry of Environment and Natural Resources, Nuuk, Greenland, 429 pp.

Box, J., D. H. Bromwich, and L.-S. Bai, 2004: Greenland ice sheet surface mass balance 1991–2000: Application of Polar MM5 mesoscale model and in situ data. *J. Geophys. Res.*, 109, D16105, doi:10.1029/2003JD004451.

Essery, R. L. H., L. Li, and J. W. Pomeroy, 1999. A distributed model of blowing snow over complex terrain. *Hydrol. Processes,* 13: 2423–2438.

Fettweis, X. 2007. Reconstruction of the 1979–2006 Greenland ice sheet surface mass balance using the regional climate model MAR. *The Cryosphere*, 1: 21–40.

Grunell, A.,Hannah, D. and Lawler, D. 1996. Suspended sediment yield from glacier basins. In: Erosion and Sediment Yield: Global and regional Perspectives, Walling D.E. and Webb, B. W. (eds). *IAHS*, **236**: 97–104.

Hag, M.P., Karlsen, H.G., Bille-Hansen, J. and Bøggild, C.E., 2002. Time trend in runoff and climatology from an ice-sheet margin catchment in West Greenland. In: Å. Killingtveit (Editor), XXII Nordic Hydrological Conference. Nordic Association for Hydrology, Røros, Norway, pp. 581–588.

Hallet, B., Hunter, L. and Bogen, J. 1996. Rates of erosion and sediment evacuation by glaciers: a review of field data and their implications. *Global Planet Change*, 12: 213–235.

Hanna, E., J. Cappelen, X. Fettweis, P. Huybrechts, A. Luckman, M. H. Ribergaard 2009. Hydrologic response of the Greenland Ice sheet: the role of oceanographic warming. *Hydrological Processes*, 23: 7–30.

Hansen, B. U., C. Sigsgaard, L. Rasmussen, J. Cappelen, J. Hinkler, S. H. Mernild, D. Petersen, M. Tamstorf, M. Rasch, and B. Hasholt, 2008. Present Day Climate at Zackenberg. *Advances in Ecological Research*, 40: 115–153.

Hasholt, B. N. Bobrovitskaya, J. Bogen, J. McNamara, S. H. Mernild, D. Milburn, and D. E. Walling, 2006. Sediment transport to the Arctic Ocean and adjoining cold oceans. *Nordic Hydrology*, 37(4–5): 413–432.

Hasholt, B. and Mernild, S. H. 2006. Glacial erosion and sediment transport in the Mittivakkat Glacier catchment, Ammassalik Island, Southeast Greenland, 2005. *IAHS* Publ. 306, pp 45–55.

Hasholt, B. and Mernild S. H. 2009. Runoff and Sediment Transport Observations from the Greenland Ice Sheet, Kangerlussuaq, West Greenland. 17th International Northern Research Basins Symposium and Workshop Iqaluit-Panqnirtung-Kuujiuaq, Canada, August 12 to 18, pp. 1–8.

IPCC, 2007: Summary for Poicymakers. In: Climate Change 2007. The Physical Science Basis. Contribution of Working Group I to the Fourth Assessment Report of the Intergovernmental Panel on Climate Change [Solomon, S., D. Qin, M. Manning, Z. Chen, M. Marquis, K.B.

Averyt, M.Tignor and H.L. Miller (eds.)]. Cambridge University Press, Cambridge, United Kingdom and New York, USA.

Janssens, I., and P. Huybrechts, 2000. The treatment of meltwater retention in mass-balance parameterisation of the Greenland Ice Sheet. *Ann. Glaciol.*, 31: 133–140.

Johannessen, O. M., K. Khvorostovsky, M. W. Miles, and L. P. Bobylev, 2005. Recent ice sheet growth in the interior of Greenland, *Sciencexpress*, 1013–1016, doi:10.1126/science.1115356.

Krabill, W. E., and Coauthors, 2000. Greenland ice sheet: Highelevation balance and peripheral thinning. *Science,* 289: 428–430.

Krabill W., E. Hanna, P. Huybrechts, W. Abdalati, J. Cappelen, B. Csatho, E. Frederick, S. Manizade, C. Martin, J. Sonntag, R. Swift, R. Thomas, and J. Yunge, 2004. Greenland Ice Sheet: Increased coastal thinning, *Geophys. Res. Lett.*, 31, L24402, doi:10.1029/2004GL021533.

Liston G. E. 1995. Local Advection of Momentum, Heat, and Moisture during the Melt of Patchy Snow Covers. *Journal of Applied Meteorology* 34(7): 1705–1715.

Liston, G. E., and K. Elder, 2006a. A distributed snow-evolution modeling system (SnowModel). *Journal of Hydrometeorology*, 7: 1259–1276.

Liston, G. E., and K. Elder, 2006b. A meteorological distribution system for high resolution terrestrial modeling (MicroMet). *Jounal of Hydrometeorology*, 7: 217–234.

Liston, G. E., and D. K. Hall, 1995. An energy-balance model of lake-ice evolution. *J. Glaciol.*, 41: 373–382.

Liston, G. E., R. B. Haehnel, M. Sturm, C. A. Hiemstra, S. Berezovskaya, and R. D. Tabler, 2007. Simulating complex snow distributions in windy environments using SnowTran-3D. *Journal of Glaciology*, 53: 241–256.

Liston, G. E., and C. A. Hiemstra, 2008. A simple data assimilation system for complex snow distributions (SnowAssim). *J. Hydrometeorology*, 9: 989–1004.

Liston, G. E., C. A. Hiemstra, K. Elder, and D. W. Cline, 2008. Meso-cell study area (MSA) snow distributions for the Cold Land Processes Experiment (CLPX). *J. Hydrometeorology*, 9: 957–976.

Liston, G. E., and M. Sturm, 1998. A snow-transport model for complex terrain. *J. Glaciol.* 44: 498–516.

Liston, G. E., and M. Sturm, 2002. Winter Precipitation Patterns in Arctic Alaska Determined from a Blowing-Snow Model and Snow-Depth Observations. *Journal of Hydrometeorology,* vol. 3: 646–659.

Liston, G. E., and M. Sturm, 2004. The role of winter sublimation in the Arctic moisture budget. *Nordic Hydrology*, 35(4): 325–334.

Liston, G. E., J.-G. Winther, O. Bruland, H. Elvehøy, and K. Sand, 1999. Below surface ice melt on the coastal Antarctic ice sheet. *J. Glaciol.*, 45(150): 273–285.

McNamara, J. P. and D. L. Kane 2009. The impact of a shrinking cryosphere on the form of arctic alluvial channels. *Hydrol. Process.* 23: 159–168.

Mernild, S. H., Hasholt, B., Kane, D. L., and Tidwell, A. C. 2008a. Jökulhlaup Observed at Greenland Ice Sheet. *Eos Trans. AGU*, 99(35): 321–322.

Mernild, S. H. and G. E. Liston, 2009. The influence of air temperature inversion on snow melt and glacier surface mass-balance simulations, SW Ammassalik Island, SE Greenland. Accepted *Journal of Applied Meteorology and Climate*.

Mernild, S. H., G. E. Liston, and B. Hasholt, 2007. Snow-Distribution and Melt Modeling for Glaciers in Zackenberg River Drainage Basin, NE Greenland. *Hydrological Processes*. 21: 3249–3263. DOI: 10.1002/hyp.6500.

Mernild, S. H., G. E. Liston, B. Hasholt, and N. T. Knudsen, 2006a. Snow distribution and melt modeling for Mittivakkat Glacier, Ammassalik Island, SE Greenland. *J. Hydrometeor.*, 7: 808–824.

Mernild, S. H., G. E. Liston, C. A., Hiemstra, and K. Steffen, 2008b. Surface Melt Area and Water Balance Modeling on the Greenland Ice Sheet 1995–2005. *Journal of Hydrometeorology*, 9(6): 1191–1211. doi: 10.1175/2008JHM957.1.

Mernild, S. H., B. Hasholt, G. E. Liston, and M. van den Broeke 2009d. Runoff simulations from the Greenland Ice Sheet at Kangerlussuaq from 2006/07 to 2007/08, West Greenland. In review *Water Resources Research.*

Mernild, S. H., G. E. Liston, C. A. Hiemstra, and K. Steffen, 2009a. Record 2007 Greenland Ice Sheet surface melt-extent and runoff. *Eos Trans. AGU*, 90(2): 13–14.

Mernild, S. H., G. E. Liston, C. A. Hiemstra, K. Steffen, E. Hanna, and J. H. Christensen, 2009b. Greenland Ice Sheet surface mass-balance modeling and freshwater flux for 2007, and in a 1995–2007 perspective. *Hydrological Processes*, DOI: 10.1002/hyp.7354.

Mernild, S. H., G. E. Liston, K. Steffen, and P. Chylek 2009c. Meltwater flux and runoff modeling in the ablation area of the Jakobshavn Isbræ, West Greenland. In review *Journal of Glaciology*.

Mote, T. L. 2007. Greenland surface melt trends 1973–2007: Evidence of a large increase in 2007, *Geophys. Res. Lett., 34,* L22507, doi:10.1029/2007GL031976.

Pomeroy, J. W., and R. L. H. Essery, 1999. Turbulent fluxes during blowing snow: Field test of model sublimation predictions. *Hydrol. Processes,* 13: 2963–2975.

Pomeroy, J. W., and D. M. Gray, 1995. Snowcover accumulation, relocation and management. National Hydrology Research Institute Science Rep. 7, Hydrological Science Division, HNRI Division of Hydrology, University of Saskatchewan, 144 pp.

Richardson, K., W. Steffen, H. Schellnhuber, J. Alcamo, T. Barker, D. Kammen, R. Leemans, D. Liverman, M. Munasinghe, B. Osman-Elasha, N. Stern, O. Waever 2009. Climate Change: Global Risks, Challenges and Decisions, Synthesis Report, Copenhagen, 10–12 March, University of Copenhagen, pp. 39.

Roberts, M. J. 2005. Jökulhlaups: A reassessment of floodwater flow through glaciers, *Rev. Geophys., 43*, RG1002, doi:10.1029/2003RG000147.

Scambos, T. and T. Haran 2002. An image-enhanced DEM of the Greenland Ice Sheet. *Annals of Glaciology*, 34: 291–298.

Serreze, M. C. and R. G. Barry, 2005. The Arctic Climate System. Cambridge Atmospheric and Space Science Series: Cambridge; p. 424.

Schmidt, R. A., 1972. Sublimation of wind-transported snow—A model. Research Paper RM-90, Rocky Mountain Forest and Range Experiment Station, Forest Service, U.S. Department of Agriculture, Fort Collins, CO, 24 pp.

Schmidt, R. A., 1982. Vertical profiles of wind speed, snow concentration, and humidity in blowing snow. *Bound.-Layer Meteor.*, **23,** 223–246.

Steffen, K. and J. Box, 2001. Surface climatology of the Greenland Ice Sheet: Greenland climate network 1995–1999. *Journal of Geophysical Research*, 106(24): 33951–33964.

Sugden, D. E., C. M. Clapperton, and P. G. Knight, 1985. A Jökulhlaup near Sønder Strømfjord, West Greenland, and some effects on the Ice-Sheet margin. *Journal of Glaciology*, **31**(109): 366–368.

Syvitski, J. P. M. 2002. Sediment discharge variability in Arctic rivers: implications for a warmer future. *Polar Research* **21**: 323–330.

Tabler, R. D., 1975. Estimating the transport and evaporation of blowing snow. *Proc. Great Plains Agricultural Council: SnowManagement on the Great Plains Symp.,* Bismarck, ND, Publication 73, 85–104.

Tedesco, M. 2007. A new record in 2007 for melting in Greenland, *Eos Trans. AGU, 88*(39), 383.

van den Broeke, M., P. Smeets, J. Ettema, and P. K. Munneke 2008a. Surface radiation balance in the ablation zone of the west Greenland ice sheet. *J. Goephys. Res.*, 113,D13105, doi:10.1029/2007/JD009283.

van den Broeke, M., P. Smeets, J. Ettema, C. van der Veen, R. van de Wal, and J. Oerlemans 2008b. Partitioning of melt energy and meltwater fluxes in the ablation zone of the west Greenland ice sheet. *The Cryosphere*, 2: 179–189.

van den Broeke, M., P. Smeets, and J. Ettema 2008c. Surface layer climate and turbulent exchange in the ablation zone of the west Greenland ice sheet. *International Journal of Climatology*. DOI: 10.1002/joc.1815.

van de Wal, R. S. W., W. Greuell, M. R. van den Broeke, C. H. Reijmer, and J. Oerlemans 2005. Surface mass-balance observations and automatic weather station data along a transect near Kangerlussuaq, West Greenland. *Annals of Glaciology*, 42: 311–316.

Woo M-K, A. G. Lewkowicz, W. R. Rouse 1992. Response of the Canadian permafrost environment to climatic change. *Physical Geography* 13: 287–317.

Yang, D., S. Ishida, B. E. Goodison, and T. Gunther, 1999. Bias correction of precipitation data for Greenland. *Journal of Geophysical Research-Atmospheres*, 104, (D6): 6171–6181.

Zwally, J. H., W. Abdalati, T. Herring, K. Larson, J. Saba, and K. Steffen, 2002. Surface melt-induced acceleration of Greenland ice-sheet flow. *Science*, 297: 218–222.

Zwally, J. H., and M. B. Giovinetto, 2001: Balance mass flux and ice velocity across the equilibrium line in drainage systems of Greenland. *J. Geophys. Res.*, 106 (33), 717–728.

Figure 1: *(a) Greenland including the Kangerlussuaq drainage area (6,130 km^2) in West Greenland; (b) simulation area with topography (gray shades elevation), the four meteorological stations: Station K (50 m a.s.l.), S5 (490 m a.s.l.), S6 (1,020 m a.s.l.), and S9 (1,520 m a.s.l.), the hydrometric station at the catchment outlet, and the catchment watershed divide. The catchment watershed divide was established in River Tools.*

Figure 2: *Relations between observed 2008 suspended sediment concentrations (SSC) and observed discharge at different distances upstream from the Kangerlussuaq catchment outlet. The R^2 value of 0.81 ($p<0.01$) is based on samples at the outlet underneath the Watson Bridges, and the 0.03 ($p<0.10$) on riverbank samples 150 and 700 m upstream.*

Figure 3: *(a) Kangerlussuaq net precipitation, runoff, and change in storage (ΔS; SMB) series for 1978/79 through 2007/08. For 2007 and 2008, the observed June through August runoff is further illustrated based on data from Mernild et al. (2009d); (b) percentage of catchment runoff explained by GrIS runoff and by precipitation and snowmelt; and (c) relationship between GrIS runoff and Kangerlussuaq catchment runoff.*

Figure 4: *(a and b) Time series of daily modeled runoff for the Kangerlussuaq part of the GrIS and for the Kangerlussuaq drainage area for 1991/92 (the year with the lowest annual cumulative runoff) and 2006/07 (highest cumulative runoff); and (c and d) time series of daily*

modeled suspended sediment load for the Kangerlussuaq drainage area for 1991/92 and 2006/07. The period from September through August follows the fixed GrIS mass-balance year.

Figure 5: *(a) Time series of Kangerlussuaq simulated runoff and passive microwave satellite-derived GrIS total melt extent area (satellite data provided by CIRES, University of Colorado at Boulder) for 1979 through 2008; and (b) relation between satellite-derived GrIS total melt area and Kangerlussuaq catchment runoff.*

Figure 6: *Time series of modeled suspended sediment load from the Kangerlussuaq drainage area for 1978/79 through 2007/08. For 2007 and 2008, the observed suspended sediment load (end of May through August) is further illustrated based on data from Mernild and Hasholt (2009).*

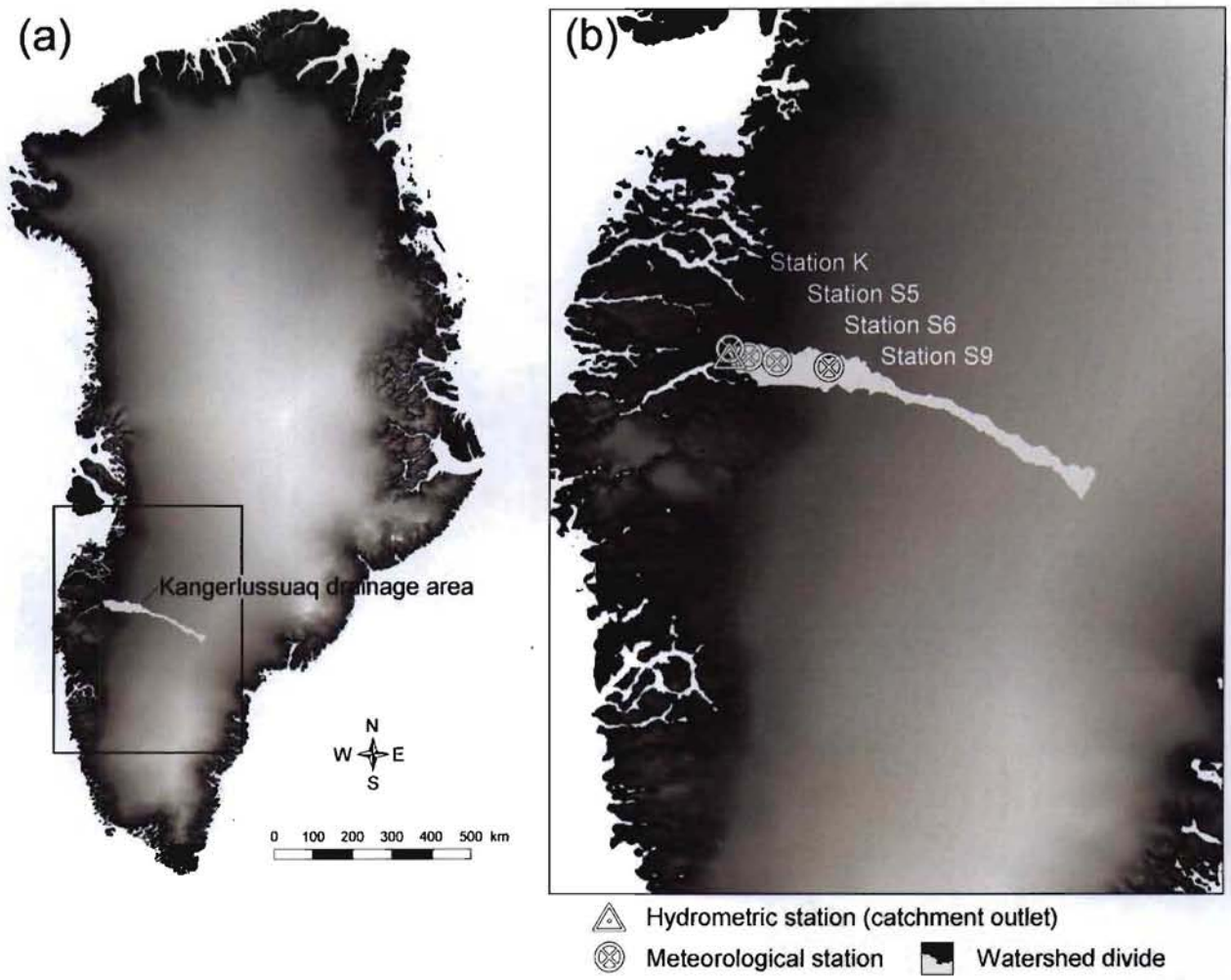

Figure 1: *(a) Greenland including the Kangerlussuaq drainage area (6,130 km^2) in West Greenland; (b) simulation area with topography (gray shades elevation), the four meteorological stations: Station K (50 m a.s.l.), S5 (490 m a.s.l.), S6 (1,020 m a.s.l.), and S9 (1,520 m a.s.l.), the hydrometric station at the catchment outlet, and the catchment watershed divide. The catchment watershed divide was established in River Tools.*

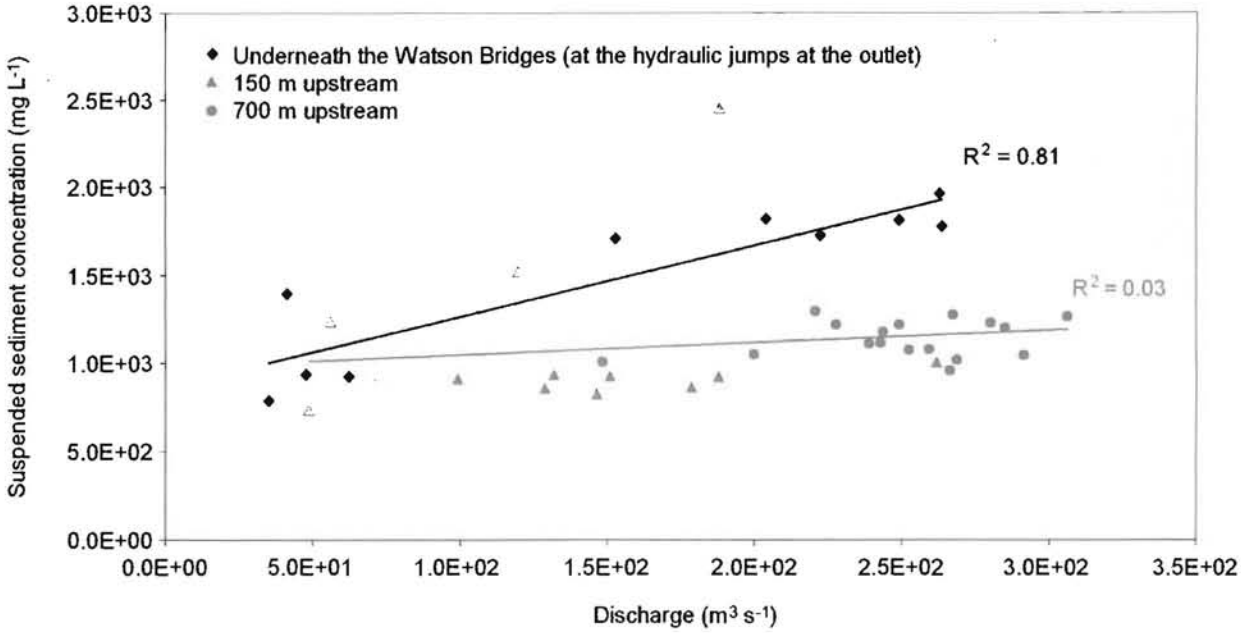

Figure 2: *Relations between observed 2008 suspended sediment concentrations (SSC) and observed discharge at different distances upstream from the Kangerlussuaq catchment outlet. The R^2 value of 0.81 ($p<0.01$) is based on samples at the outlet underneath the Watson Bridges, and the 0.03 ($p<0.10$) on riverbank samples 150 and 700 m upstream.*

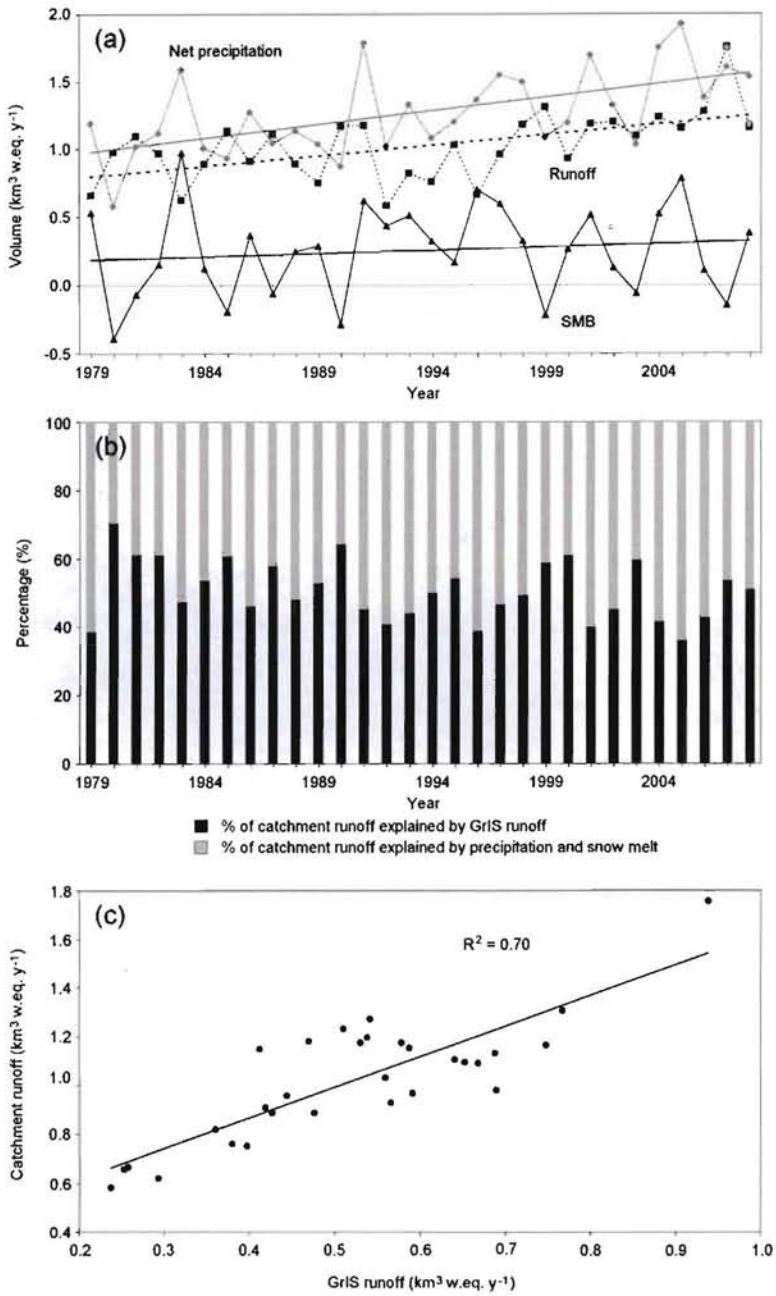

Figure 3: *(a) Kangerlussuaq net precipitation, runoff, and change in storage (ΔS; SMB) series for 1978/79 through 2007/08. For 2007 and 2008, the observed June through August runoff is further illustrated based on data from Mernild et al. (2009d); (b) percentage of catchment runoff explained by GrIS runoff and by precipitation and snowmelt; and (c) relationship between GrIS runoff and Kangerlussuaq catchment runoff.*

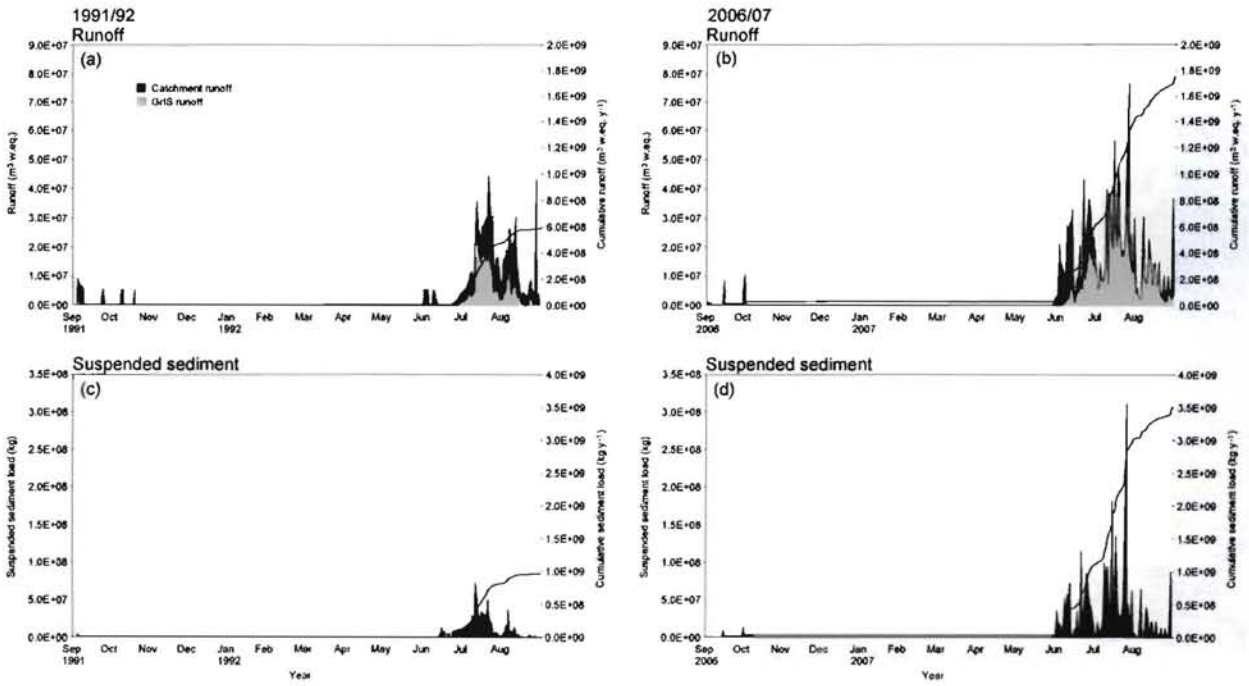

Figure 4: *(a and b) Time series of daily modeled runoff for the Kangerlussuaq part of the GrIS and for the Kangerlussuaq drainage area for 1991/92 (the year with the lowest annual cumulative runoff) and 2006/07 (highest cumulative runoff); and (c and d) time series of daily modeled suspended sediment load for the Kangerlussuaq drainage area for 1991/92 and 2006/07. The period from September through August follows the fixed GrIS mass-balance year.*

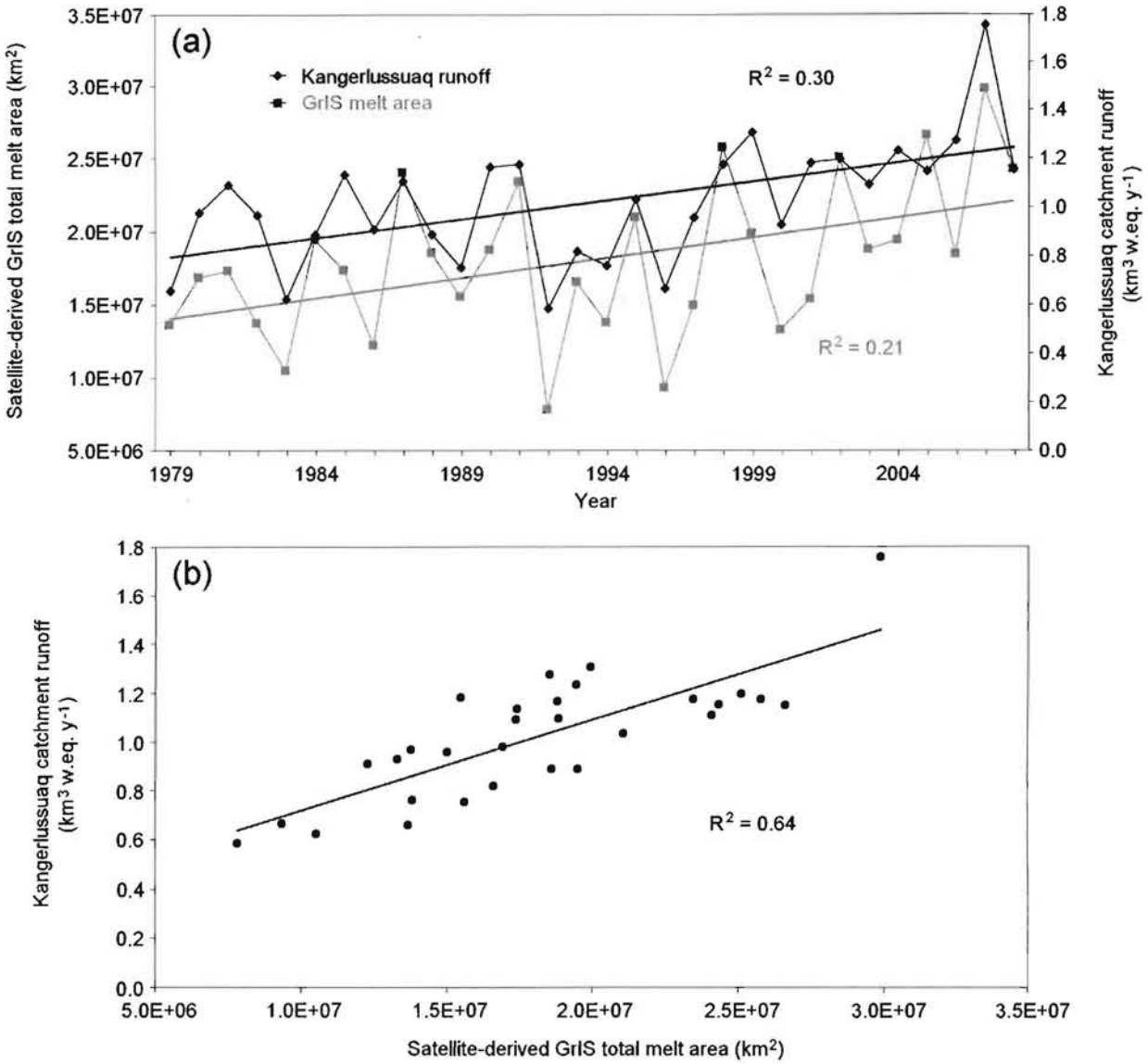

Figure 5: *(a) Time series of Kangerlussuaq simulated runoff and passive microwave satellite-derived GrIS total melt extent area (satellite data provided by CIRES, University of Colorado at Boulder) for 1979 through 2008; and (b) relation between satellite-derived GrIS total melt area and Kangerlussuaq catchment runoff.*

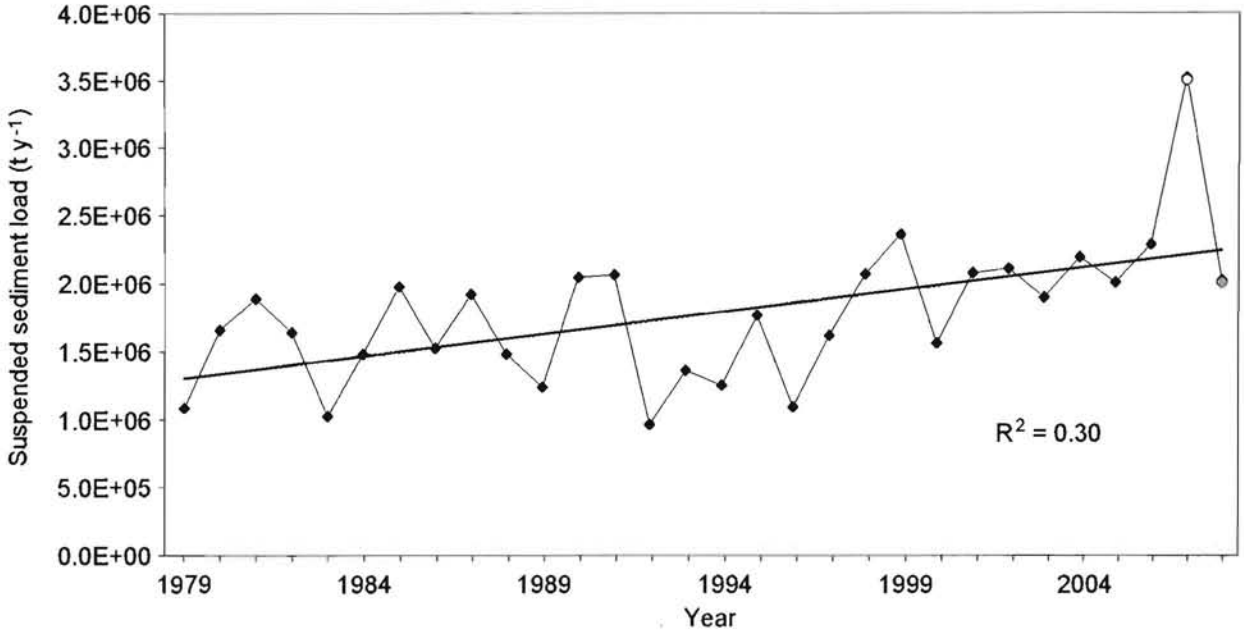

Figure 6: *Time series of modeled suspended sediment load from the Kangerlussuaq drainage area for 1978/79 through 2007/08. For 2007 and 2008, the observed suspended sediment load (end of May through August) is further illustrated based on data from Mernild and Hasholt (2009).*

Table 1: *Meteorological input data for the Kangerlussuaq simulations. Meteorological station data on the GrIS (S5, S6, and S9) were provided by Utrecht University, and coastal meteorological station data (K; Kangerlussuaq) by the Danish Meteorological Institute (DMI). For further information about the S-stations see e.g., van den Broeke et al. (2008).*

Meteorological station name	Location	Grid	Data time period for runoff simulations	Altitude (m a.s.l.)	Parameters
K	Town Kangerlussuaq	67°01′N, 50°42′W[†]	1 Sep 1979 – 31 Aug 2008	50	Air temperature, relative humidity, wind speed, wind direction, and corrected precipitation
S5	Ice Sheet	67°06′N, 50°07′W	1 Sep 2006 – 31 Aug 2007	490	Air temperature, relative humidity, and wind speed
S6	Ice Sheet	67°05′N, 49°23W	1 Sep 2006 – 31 Aug 2007	1,020	Air temperature, relative humidity, and wind speed
S9	Ice Sheet	67°03″N, 48°14′W	1 Sep 2006 – 31 Aug 2007	1,520	Air temperature, relative humidity, and wind speed

[†] The meteorological station in Kangerlussuaq was moved 660 m, with no change in elevation, in 2004, to the present location at the airport (50 m a.s.l.) (pers. com. Juncher Jensen, Danish Meteorological Institute). No air temperature correction was made to the Kangerlussuaq meteorological data.

Table 2: *User-defined constants used in the SnowModel simulations (see Liston and Sturm (1998) for parameter definitions).*

Symbol	Value	Parameter
C_v		Vegetation snow-holding depth (equal surface roughness length) (m)
	0.50	- Barren bedrock/vegetation
	0.50	- River valley
	0.01	- Ice/snow
F	500.0	Snow equilibrium fetch distance (m)
U_{*_t}	0.25	Threshold wind-shear velocity (m s^{-1})
Z_0	0.01	Snow surface roughness length (m)
dt	1	Time step (daily and hourly)
$dx = dy$		Grid cell increment (km)
	0.5	- Greenland Ice Sheet Kangerlussuaq simulation area
α		Surface albedo
	0.5–0.8	- Snow (variable snow albedo according to surface snow characteristics)
	0.4	- Ice
ρ		Surface density (kg m^{-3})
	280	- Snow
	910	- Ice
ρ_s	550	Saturated snow density (kg m^{-3})

***Table 3**: Rank-ordered Kangerlussuaq catchment net precipitation (defined as P–(SU+E)), runoff (R), change in storage (ΔS; SMB), suspended sediment load, and catchment summer (June, July, and August) air temperature anomaly for 1978/79 through 2007/08.*

Rank	Net precipitation (N-(SU+E)) (km^3 w.eq. y^{-1})	Runoff (R) (km^3 w.eq. y^{-1})	Change in storage (ΔS; SMB) (km^3 w.eq. y^{-1})	Suspended sediment load ($\times 10^6$ t y^{-1})	Catchment summer air temperature anomaly (JJA) (°C)
1	1.93 (2004/05)	1.76 (2006/07)	0.97 (1982/83)	3.52 (2006/07)	1.89 (2003)
2	1.79 (1990/91)	1.31 (1998/99)	0.78 (2004/05)	2.36 (1998/99)	1.58 (2000)
3	1.76 (2003/04)	1.27 (2005/06)	0.70 (1995/96)	2.29 (2005/06)	1.43 (2001)
4	1.70 (2000/01)	1.23 (2003/04)	0.62 (1990/91)	2.19 (2003/04)	1.42 (2007)
5	1.61 (2006/07)	1.20 (2001/02)	0.60 (1996/97)	2.11 (2001/02)	1.13 (2008)
26	1.02 (1980/81)	0.75 (1988/89)	-0.14 (2006/07)	1.24 (1980/81)	-1.08 (1996)
27	1.01 (1983/84)	0.67 (1995/96)	-0.19 (1984/85)	1.09 (1995/96)	-1.53 (1979)
28	0.94 (1984/85)	0.66 (1978/79)	-0.22 (1998/99)	1.08 (1978/79)	-1.90 (1992)
29	0.88 (1989/90)	0.62 (1982/83)	-0.29 (1989/90)	1.02 (1982/83)	-2.89 (1983)
30	0.59 (1979/80)	0.58 (1991/92)	-0.39 (1979/80)	0.96 (1991/92)	-3.18 (1982)
30-year average and standard deviation	1.28(±0.31)	1.02(±0.25)	0.26(±0.34)	1.77(±0.52)	0.00(±1.26)